A&A 391, 705–711 (2002)
DOI: 10.1051/0004-6361:20020855
© ESO 2002

Astronomy & Astrophysics

Interstellar NaI and CaII absorption observed towards the Cygnus Loop SNR

B. Y. Welsh[1], S. Sallmen[1], D. Sfeir[1], and R. Lallement[2]

[1] Experimental Astrophysics Group, Space Sciences Laboratory, UC Berkeley, Berkeley, CA 94720, USA
[2] Service Aeronomie du CNRS, 91371 Verrieres-le-Buisson, France

Received 17 April 2002 / Accepted 6 Juin 2002

Abstract. We present high resolution spectra ($R \sim 5$ km s^{-1}) of the interstellar NaI and CaII absorption lines observed towards 9 early-type stars with distances ranging from 250 to 2300 pc in the line-of-sight towards the Cygnus Loop Supernova Remnant (SNR). All but one of these absorption profiles can be fit using a combination of one or more of three absorption components with average best-fit (lsr) velocities of $V_1 = +0.8$ km s^{-1}, $V_2 = +9.0$ km s^{-1} and $V_3 = +19.7$ km s^{-1}. An additional velocity component at $V_4 = +29.7$ km s^{-1} is required in order to fit the NaI profile recorded towards the star HD 198946, whose distance of 794 pc places it well in excess of the nominal 440 pc distance to the SNR. The NaI/CaII column density ratios for the three higher velocity components are typically <1.0, which are similar to values found for high-velocity gas components detected towards other evolved SNRs. Even though we have detected the three higher velocity components solely along the sight-lines towards stars with distance estimates greater than that of the Cygnus Loop, we are unable to definitely associate these components with an interaction between the expansion of the SN shock wave and the ambient interstellar medium. We suggest a more likely origin for these absorption components is that of an old pre-cursor SN neutral gas shell, within whose interstellar cavity the Cygnus Loop supernova explosion occured some 20 000 years ago.

Key words. ISM: supernova remnants – ISM: atoms

1. Introduction

A large proportion of the energy released in a supernova (SN) explosion is deposited in the kinetic energy of the ejecta which subsequently interacts with the ambient interstellar gas. This blast wave governs mass exchange between various phases of the interstellar medium (ISM) and thus SNe greatly influence subsequent star formation rates and the recycling of heavy elements in galaxies. The spectral signatures (in both emission and absorption) of the low density disturbed interstellar gas surrounding a SNR are best sampled in the ultraviolet region which contains spectral lines covering a wide range of ionization stages from a large variety of elements. High-velocity shocked interstellar gas at velocities in excess of ~75 km s^{-1} has thus far been observed in absorption for only three galactic supernova remnants (SNRs); the Vela SNR (Jenkins et al. 1984), the Monoceros Loop (Welsh et al. 2001) and Shajn 147 (Gondhalekar & Phillips 1980). These absorption studies have successfully combined data from both the ultraviolet and visible regime to provide a detailed analysis of the velocities, masses, densities, pressures and elemental depletion of the disturbed gas in the vicinity of these SNRs. Although two other optically bright SNRs (the Cygnus Loop and Puppis-A) have been extensively studied in *emission* at visible, UV and X-ray wavelengths (Graham et al. 1995; Blair et al. 1995), surprisingly (until this Paper) no suitable background stellar continuum sources had been discovered for either of these SNRs to allow their (expected) disturbed ambient gas to be studied at high spectral resolution in absorption.

The Cygnus Loop SNR is probably one of the most observed SNRs since it has a large apparent size ($2.8° \times 3.5°$), has a high surface brightness and it is relatively unobscured with a low reddening of $E(B-V) \sim 0.08$. It is an evolved remnant of middle age (~20 000 years) that was formed by an explosion within a pre-existing cavity which is thought to be surrounded by a high-density shell of interstellar gas (Levenson et al. 1998). The SN blast wave has only recently begun to impinge on its surrounding medium and the interaction of the outflowing SN shock with the complex edges of the dense cavity wall is responsible for the contorted filamentary structures revealed by observations of both optical and X-ray emission (Danforth et al. 2000). Visible and ultraviolet emission studies predict a shock with a velocity of ~170 km s^{-1} that is being driven into an inhomogenous, partly neutral ambient interstellar medium (Sankrit et al. 2000; Danforth et al. 2000), while X-ray data suggest hot shocked gas with a higher velocity of ~400 km s^{-1} (Ku et al. 1984).

Blair et al. (1999) have recently determined a new distance of 440 ± 100 pc to this SNR (as opposed to the previously accepted distance of 770 pc), which presented us with

Send offprint requests to: B. Y. Welsh,
e-mail: bwelsh@ssl.berkeley.edu

Article published by EDP Sciences and available at http://www.aanda.org or http://dx.doi.org/10.1051/0004-6361:20020855

the opportunity to use the Hipparcos Catalog of stellar distances (ESA 1997) to search for suitable background targets that could be used as possible interstellar absorption probes of the SNR. Using the X-ray and H-α emitting boundary of the SNR as detailed by Levenson et al. (1998), we searched for potential early-type (O, B and A) stars with distances >250 pc that lay within these contours and carried out observations of the interstellar lines of NaI and CaII towards these targets to search for any absorption components that could be associated with the expansion of the SNR. Both of these visible interstellar lines sample mainly neutral interstellar material, and they have been successfully used both by Wallerstein & Silk (1971) in detecting high-velocity gas associated with the Vela SNR and also by Silk & Wallerstein (1973) in similar observations of the Shajn 147 SNR.

In this Paper we present high resolution ($R \sim 5$ km s^{-1}) observations of the NaI and CaII interstellar absorption lines for 9 stellar targets in lines-of-sight towards the Cygnus Loop SNR that have distance estimates ranging from ~250 to 2300 pc. The pattern of absorption seen towards the two stars with Hipparcos distances less than the canonical 440 pc to the Cygnus Loop SNR is best fit by a single absorbing gas cloud with a velocity of $V_{\rm lsr} = +0.8$ km s^{-1}. For targets with distances greater than that of the SNR we have observed up to 3 additional higher velocity absorption components at $V_2 = +9.0$ km s^{-1}, $V_3 = +19.7$ km s^{-1} and $V_4 = +29.7$ km s^{-1}. Finally, we discuss the possible origin of these higher velocity components and their association with the Cygnus Loop SNR.

2. Observations and data processing

In Table 1 we list the 9 observed stellar targets together with their galactic position, visual magntitude ($M_{\rm v}$), spectral type and distance estimate. Hipparcos satellite distances are available for four of the stars and are marked by an asterix (*) in Table 1. For four of the remaining five targets we have estimated the stellar distance in the following two ways in order to bracket the minimum and maximum distance range for these targets: (i) a minimum photometric distance was derived using the published spectral types, the absolute magnitude classifications given in Humphreys & McElroy (1984) and Balona & Crampton (1972) and an assumed reddening value of $E(B-V) = 0.08$, and (ii) a maximum distance estimate was based on scaling to the visual magnitude of a nearby star(s) of the same spectral type (A0V or B9V) and known Hipparcos distance (in this case the reddening values are assumed to be identical for each target pair). For the star HD 197702 (B1 III) we have obtained a photometric distance of ~2.3 kpc under the assumption of a reddening value of $E(B-V) = 0.08$. We shall return to the question of the relative accuracy of these distance estimates in the Sect. 4 in light of the pattern of interstellar absorption observed towards these stars.

Figure 1 displays the positions of all nine stars with respect to the H-α emission map of the Cygnus Loop of Levenson et al. (1998), which tracks the expansion boundary of ionized gas of the SNR. The star HD 198056 has an accurate Hipparcos distance of 292 pc, and thus can be used as a foreground reference when comparing the absorption characteristics of the remaining 8 lines-of-sight. The star HD 197702 is the most distant at ~2300 pc and (as will be shown later) its sight-line most probably samples the outer regions of the H-α and X-ray emission boundary to the SNR.

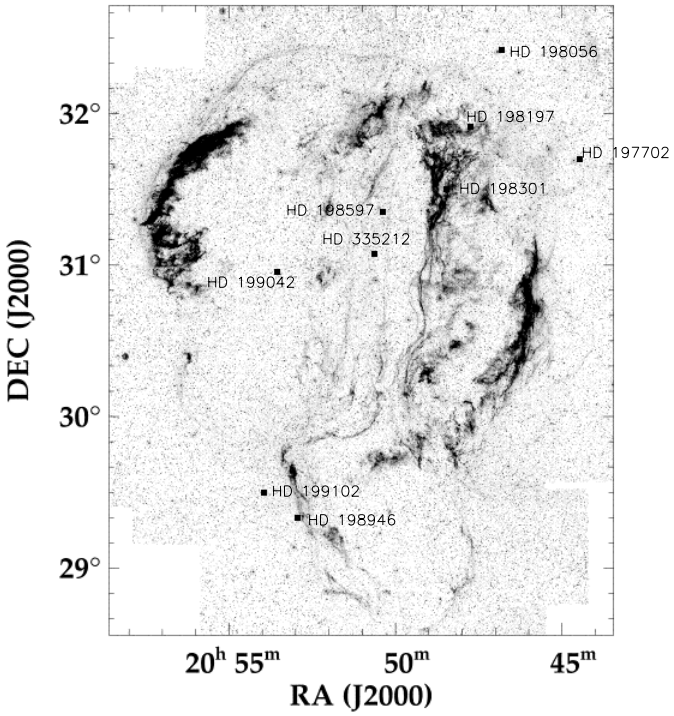

Fig. 1. H-α emission contour map of the Cygnus Loop SNR (Levenson et al. 1998) showing the positions of the 9 early-type stars observed in the interstellar absorption lines of NaI and CaII.

Observations of the interstellar NaI D-lines at ~5890 Å and the interstellar CaII K-line at 3933 Å were obtained during two observing runs. Three of the stars (HD 198301, HD 198946 and HD 199042) were observed during the nights of August 24–26th, 2001 using the Aurelie echelle spectrograph at the 1.52 m telescope of the Observatoire de Haute Provence (France). These data were supplemented by interstellar absorption observations of the remaining six stars using the Hamilton echelle spectrograph on the coude feed telescope at the Lick Observatory (USA) on May 23rd, 2001.

The raw spectral data were reduced in a similar manner to that described in Sfeir et al. (1999), which includes detector flatfield and background corrections. Wavelength calibration of the spectra was obtained using a Th-Ar calibration lamp spectrum, which resulted in a wavelength accuracy of ~0.015 Å (1.0 km s^{-1}). The resolution of the Observatoire de Haute Provence data was determined to be 3.0 km s^{-1} and that of Lick Observatory data was 5.5 km s^{-1}. All the NaI spectra were well-exposed with typical S/N ratios in excess of 50:1. The CaII data were generally less well-exposed with S/N ratios of ~30:1, except for the stars HD 198197 and HD 335212 which had very low S/N ratios of only ~5:1.

Equivalent widths of the interstellar NaI and CaII lines are given in Table 1 together with estimates of their associated measurement errors. The residual intensity spectra for the NaI and CaII lines for all the target stars are shown in Figs. 2 and 3.

Table 1. Stellar target information and equivalent width measurements.

Star	(l, b)	M_v	Sp	distance (pc)	NaI D-2 (mÅ)	NaI D-1 (mÅ)	CaII-K (mÅ)
HD 197702	(73.9°,−6.8°)	7.9	B1III	2300	480 ± 35	450 ± 35	350 ± 30
HD 198056	(74.8°,−6.8°)	7.0	B9V	292*(+69,–46)	105 ± 10	67 ± 10	55 ± 8
HD 198197	(74.5°,−7.2°)	7.8	A0V	658*(+1000,–250)	140 ± 25	125 ± 25	80 ± 30
HD 198301	(74.8°,−6.8°)	8.65	A0V	345–800	320 ± 30	230 ± 25	170 ± 15
HD 198597	(74.4°,−8.0°)	7.7	A0V	331*(+60,–80)	145 ± 15	130 ± 10	40 ± 8
HD 198946	(73.2°,−9.7°)	8.0	B9V	794*(+1478,–300)	240 ± 25	195 ± 20	85 ± 10
HD 199042	(74.6°,−8.8°)	7.8	B9V	270–600	325 ± 25	240 ± 25	85 ± 15
HD 199102	(73.5°,−9.8°)	7.6	B9V	250–440	215 ± 20	180 ± 20	100 ± 15
HD 335212	(74.3°,−8.3°)	8.8	A0V	370–910	200 ± 30	170 ± 30	130 ± 35

** = Hipparcos distance*

3. Interstellar analysis

Inspection of the interstellar NaI and CaII profiles shown in Figs. 2 and 3 reveals appreciable velocity structure for most of the lines-of-sight sampled. However for both HD 198056 (d = 292 pc) and HD 198597 (d = 331 pc), the two stars closest to the Sun and presumably foreground to the SNR, the pattern of absorption for both the NaI and CaII lines is best fit with a single absorbing cloud with velocity, $V_{\rm lsr} \sim +1$ km s^{-1}. In contrast, the stars with distances comparable to, or greater than, that of the SNR (i.e. HD 198946 (d = 794 pc), HD 198197 (d = 658 pc) and HD 198301 (d = 345−800 pc)) clearly have far more complex interstellar profiles. We identify this extra absorption with interstellar gas at a distance of 350–650 pc. In Sect. 4 we discuss whether these absorption features can be associated with the interaction between the expansion of the Cygnus Loop SNR and the ambient ISM.

We have fit the local stellar continua of all the observed NaI and CaII lines with a multi-order polynomial in order to produce the residual intensity profiles shown in Figs. 2 and 3. These interstellar profiles were then fit with one or more absorption components (which we identify as interstellar clouds) using the line-fitting program described in Sfeir et al. (1999). In brief, this entails describing each profile by a theoretical Gaussian velocity dispersion parameter, b, a cloud component LSR velocity, V, and a cloud component column density, N. The best-fit values of V, b and N for the NaI and CaII lines are listed (with their associated errors) in Table 2. We have found that all but one of the observed NaI and CaII profiles (i.e. that of HD 198946) can be fit using a combination of one or more of three absorption components with average best-fit velocities of $V_1 = +0.8$ km s^{-1}, $V_2 = +9.0$ km s^{-1} and $V_3 = +19.7$ km s^{-1}. For the purpose of our subsequent analysis and discussion, absorption components are recognized as being "common" between various target lines-of-sight if their best-fit velocity listed in Table 2 lies within ∼±3.5 km s^{-1} of these 3 velocities.

We note that an additional component (V_4) at a velocity of +29.7 km s^{-1} is required in order to fit both the NaI D1 and D2-line absorption profiles recorded towards HD 198946. Interestingly there is no corresponding absorption component detected in the CaII profile at this velocity to a detection limit of $\log N$(CaII) < 11.5 cm^{-2}. We further note that HD 198946, with a Hipparcos distance of 792 pc, is also the most distant target observed in this study that has a sight-line that clearly passes through the emission contours of the SNR shown in Fig. 1.

4. Discussion

A shock velocity of ∼170 km s^{-1} for the Cygnus Loop has been determined from H-α imaging of the Balmer filaments (Hester et al. 1994), which is in good agreement with the velocity determined from far ultraviolet observations of the OVI, NV and CIV emission lines (Long et al. 1992). However, the X-ray emission (which is dominated by emisison from the region between the main and reverse SN-driven shocks) is best described by an even greater shock of velocity ∼400 km s^{-1} (Ku et al. 1984). Although the X-rays are produced in very hot ($T \sim 10^6$ K) gas, optical and ultraviolet emission is thought to arise in slower shock regions that have cooled to $T \sim 10^4$ K. We have searched all of our profile data for absorption features that could be associated with these high-velocity shocks without any success. However our absorption data recorded towards HD 198946, the only stellar target with a distance >750 pc whose sight-line definitely passes through the H-α contours of the SNR, suggest that we may have detected disturbed interstellar regions with much slower kinetic motions, typically with a velocity difference of ∼+28 km s^{-1} with respect to the line-of-sight interstellar absorption. Thus, our present visible line absorption data would suggest that we are not sampling the same shocked gas regions that have such prominent emission (and high ionization) characteristics as observed in the ultraviolet and X-ray data.

Figure 1 clearly shows extensive filamentary (Balmer) emission that is consistent with shocks being driven by the SN blast wave into a partly neutral, ambient medium. This surrounding gas is highly inhomogenous and governs the subsequent evolution of the expansion of the SNR (Klein et al. 1994; Hester et al. 1994). Our present absorption measurements (of the NaI and CaII ions) sample interstellar gas with

Table 2. Absorption line best-fit parameters.

Star	Line	V_1 km s^{-1}	b_1	N_1 (10^{11} cm^{-2})	V_2 km s^{-1}	b_2	N_2 (10^{11} cm^{-2})	V_3 km s^{-1}	b_3	N_3 (10^{11} cm^{-2})	V_4 km s^{-1}	b_4	N_4 (10^{11} cm^{-2})
HD 197702	NaI...				+8.5	4.6	2300±1500	+22.8	1.1	3.5±0.7			
	CaII...				+6.5	8.1	55±6	+18.2	11.9	2.7±0.4			
HD 198056	NaI...	+1.0	4.3	7.3±1.0									
	CaII...	+2.3	2.6	8.0±3.0									
HD 198197	NaI...	-0.5	1.9	19.5±5.0				+17.0	1.5	2.7±1.0			
	CaII...	-2.0	8.1	11.1±5.0									
HD 198301	NaI...	+0.2	2.1	13.1±1.5	+9.0	4.1	21.8±2.0	+22.3	1.0	4.4±1.0			
	CaII...	-0.2	2.4	2.4±0.8	+7.7	4.5	10.3±2.0	+18.8	8.2	13.3±1.5			
HD 198597	NaI...	+1.0	2.2	38.8±3.0									
	CaII...	-2.8	2.0	6.6±1.5									
HD 198946	NaI...	+1.5	3.2	42.7±10				+22.0	1.0	4.4±1.0	+29.7	6.7	1.3±1.0
	CaII...	+4.6	5.6	8.3±1.0				+18.5	3.8	8.8±1.0	+28.5	N/A	<3.5
HD 199042	NaI...	+0.8	3.7	13.6±1.0	+8.0	2.7	7.1±1.0	+20.0	2.3	14.6±2.0			
	CaII...	+1.2	1.0	0.7±0.1	+9.4	7.4	8.5±2.0	+19.0	2.8	2.6±1.1			
HD 199102	NaI...	+1.2	3.6	39.4±5.0	+11.0	2.4	0.7±0.2						
	CaII...	+4.0	9.9	13.5±0.5									
HD 335212	NaI...	+1.9	2.7	35.5±15.0	+10.8	1.1	3.1±2.0	+18.3	0.9	0.8±1.0			
	CaII...	-1.0	4.8	13.7±9.0	+10.0	6.4	7.0±3.0						

an ionization potential <11.9 eV, and thus they are well-suited to the detection of a mainly neutral medium. The NaI D-lines sample gas with a temperature typically <1000 K, and since we have detected absorption components with similar velocities in both the NaI and CaII lines, we can confidently infer that all these cloud components arise in a relatively cold, mainly neutral medium. In Sect. 4.5 we will discuss whether the presently discovered higher velocity components of this neutral gas have been influenced by the expansion of the Cygnus Loop SNR.

The NaI/CaII column density ratio has been widely used as a diagnostic of the physical conditions observed throughout the diffuse ISM (Crawford 1992), with the caveat that the NaI and CaII ions observed at a similar absorption velocity may not necessarily be produced in the same physical regions of a cloud. For low velocity diffuse interstellar gas clouds characterized by $n_{\rm H} \sim 10$ cm^{-3} and $T_{\rm K} \sim 100$ K, a NaI/CaII ratio of 1–100 is typical. For the presently observed V_1 absorption component we find NaI/CaII ratios of 0.9–19.4, consistent with the absorption arising in line-of-sight diffuse interstellar gas clouds. At higher interstellar velocities the NaI/CaII density ratio has been widely observed to decrease with increasing cloud velocity (Routly & Spitzer 1952), due to the removal of adsorbed Ca atoms from interstellar grain surfaces by shocks in the higher velocity gas clouds. For most of the (higher velocity) V_2 and V_3 components presently observed towards the Cygnus SNR we find NaI/CaII ratios typically <1.0, suggesting the presence of the moderate removal of Ca from grains, presumably by low velocity interstellar shocks <20 km s^{-1}.

Before progressing to the topic of identifying the physical location and processes by which these cloud components may be formed, we will briefly discuss the absorption characteristics of each of the sight-lines to the 9 targets with reference to the data presented in Figs. 2 and 3 and Tables 1 and 2. For convenience, we discuss these absorption data with respect to four angularly close groups of stars located in the north-east, centre and south of the SNR (see Fig. 1).

4.1. HD 197702 and HD 198056

Both of these stars are located in the very outer north-eastern region of the SNR, and on first inspection of the H-α emission contours shown in Fig. 1 both would seem to possess lines-of-sight just beyond the boundary of the Cygnus Loop. The star HD 197702 is the most distant of all the 9 sight-lines sampled ($d \sim 2.3$ kpc) and both of its NaI and CaII absorption profiles exhibit (expectedly) strong line saturation. These NaI and CaII absorption profiles span the widest extent in velocity of all the targets observed in our sample (i.e. −20 to +40 km s^{-1}). Although in Table 2 we have associated the main absorption profile of HD 197702 with the V_2 component, in reality we suspect that this single component probably consists of several unresolved interstellar clouds and thus the NaI/CaII density ratio value of 41.8 derived for the V_2 component should really be viewed as a line-of-sight average. We also note the detection of the V_3 component in both the NaI and CaII lines towards this star with a NaI/CaII density ratio of 1.3. The V_3 absorption component has also been detected towards 5 other targets with sight-lines that are aligned within the SNR H-α emission boundary and also these 5 stars all have distances greater than the 440 pc to the SNR. This commonality in absorption component velocity strongly suggests that the sight-line to HD 197702 does in fact pass through the outer edge of the H-α emission contour of the SNR, and thus the observed V_3 component represents absorption from a gas cloud with a similar distance to that observed towards the other 5 targets. Since this cloud component has been detected in the absorption spectra of stars ∼3° apart on the sky, then if we assume its distance is at least 440 pc we can derive a minimum cloud size of 23 pc. This is rather large for the gas clouds commonly observed in the general ISM (McKee & Ostriker 1977), and thus it seems more likely that this absorption component may be associated in some way to the disruptive effect of the Cygnus SN on the ambient ISM.

The angularly nearby star HD 198056 is the closest to the Sun of all the observed targets (292 pc). This sight-line can definitely be considered as foreground to the SNR and its single-cloud absorption characteristics revealed by both the NaI and CaII lines confirm this viewpoint. The NaI/CaII ratio of 0.9 (which is on the low-end of ratios found for the general ISM) can be explained by an observed deficiency of interstellar NaI that can be associated with the first 100 pc of this sight-line's passage through the hot, ionized Local Bubble region (Welsh et al. 1994).

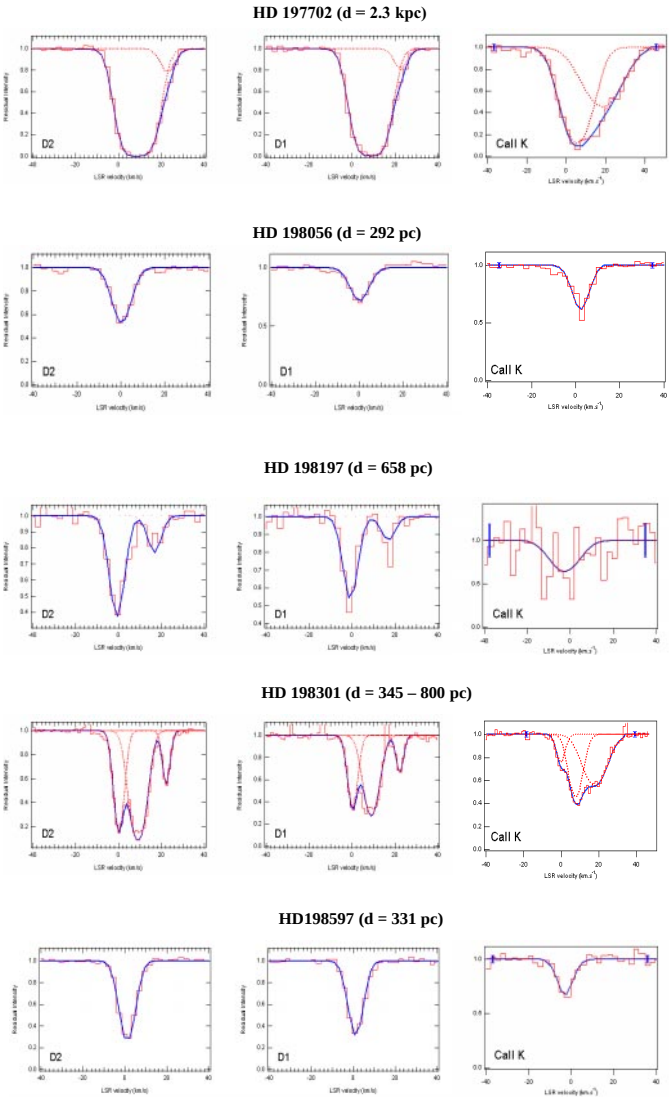

Fig. 2. Interstellar NaI D1 & D2 and CaII-K absorption line profiles and their best-fit models for the stars HD 197702, HD 198056, HD 198197, HD 198301 and HD 198597.

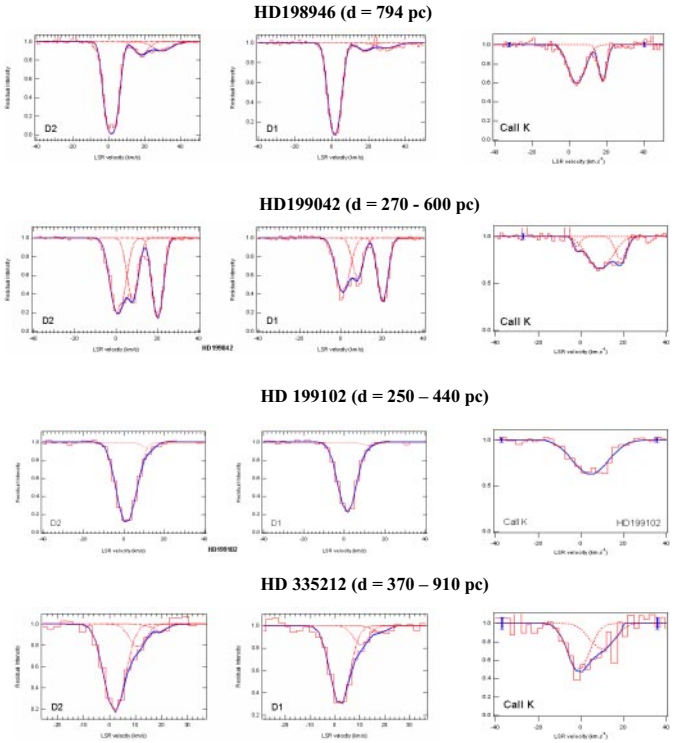

Fig. 3. Interstellar NaI D1 & D2 and CaII-K absorption line profiles and their best-fit models for the stars HD 198946, HD 199042, HD 199102 and HD 335212.

4.2. HD 198197 and HD 198301

The star HD 198197 has a Hipparcos distance of 658 pc and Fig. 1 shows that its line-of-sight clearly samples the inner (north-eastern) edge of the SNR region. We have observed two well-resolved absorption components (V_1 and V_3) in the NaI profiles, but the CaII data was of very low S/N and only the V_1 component could be confidently identified in the recorded profile. The angularly close star HD 198301 has an estimated distance range of 345–800 pc and its sight-line samples a region of strong filamentary H-α emission as shown in Fig. 1. We have detected three well-resolved absorption components (V_1, V_2 and V_3) in both the NaI and CaII lines and thus, given the similarity between the NaI profiles of HD 198197 and HD 198301, it seems likely that the actual distance to HD 198301 lies beyond the 440 pc to the SNR at a distance similar to that of HD 198197 (i.e. in the range 600–800 pc).

The NaI/CaII density ratio for the well-resolved V_3 component detected towards HD 198301 is 0.33, which is the lowest of all the ratios determined in this study. We note that the CaII absorption profile recorded towards this star extends to a velocity of +40 km s^{-1}, and although we have fit this profile with a broad V_3 component it may in fact be composed of an additional unresolved component at a velocity close to V_4.

4.3. HD 198597, HD 199042 and HD 335212

These 3 stars lie within the central region of the SNR, seemingly well away from the dense Balmer filamentary emission associated with the outer regions of the SNR. The closest of these stars is HD 198597 with a Hipparcos distance of 331 pc. Both the NaI and CaII profiles recorded to this star are of a single absorption component at $V_1 \sim 0$ km^{-1}, and thus we can be confident that this target is foreground to the remnant.

The NaI and CaII absorption profiles observed towards HD 199042 (d = 270–600 pc) are quite similar to those recorded towards HD 198301 (as discussed in 4.2), and consist of 3 well resolved velocity components. However, on closer inspection of these profiles we note that the relative strengths of the NaI components are quite different for the two stars, suggesting significant inhomogeneity in the intervening interstellar medium. For example, the V_3 component is far stronger in the NaI spectrum of HD 199042, whereas the NaI V_2 component is stronger in the spectrum of HD 198301. Interestingly, the CaII profiles of both stars have similar relative absorption

strengths between all 3 velocity components, with the absolute residual intensity values for these components in the CaII spectrum of HD 198301 being stronger by a factor of ∼2. Given the general similarity between these two star's absorption spectra we suggest that a distance of 500–600 pc is more appropriate for HD 199042.

The NaI spectrum of HD 335212 is best-fit with 3 velocity components, while its (low S/N) CaII spectrum requires only two components. Although the three-component pattern of NaI absorption is similar to that of both HD 199042 and HD 198301, the V_2 and V_3 absorption components for HD 335212 are far weaker. This could be due to inhomogeneity of both components across the SNR, or more likely could be attributed to HD 335212 being at a distance slightly less than that of the ∼600 pc to both HD 199042 and HD 198301.

4.4. HD 198946 and HD 199102

The pattern of both NaI and CaII absorption observed towards HD 199102 (d = 250–440 pc) is dominated by a single velocity component (V_1), with an additional very weak component at V_2 in the NaI profiles. Although the sight-line to this star appears to be just outside the southern limit of the H-α contours shown in Fig. 1, the detection of the weak V_2 NaI component (which has only been detected towards targets with distances >330 pc) suggests that the distance to this star may be just beyond the 440 pc to the SNR.

The star HD 198946 has a Hipparcos distance of 794 pc and its sight-line also samples the southern extension of the SNR. We have detected three well-resolved components (V_1, V_3 and V_4) in the NaI spectrum. The absence of the V_2 component can be attributed to it presently not being resolved due to the saturation of the strong V_1 component. The V_3 component is also detected in the CaII profile, such that a NaI/CaII density ratio of 0.5 can be determined for this gas cloud. We note the detection of the highest velocity, V_4, NaI component seen towards any of our 9 targets at $V_{\rm lsr}$ = +29 km s^{-1}. We have not been able to detect a corresponding component in the CaII absorption profile towards this star. However, we have estimated an upper limit of $\log N$(CaII) < 11.54 cm^{-2} for a plausible V_4 component which results in a lower limit of NaI/CaII > 0.37 for this component. A density ratio of <1.0 is consistent with values found for high-velocity components observed towards other SNRs such as the Monoceros Loop (Sfeir 1999) and the Vela SNR (Wallerstein & Silk 1971). As stated previously, in such cases the low density ratios are thought to be caused by an enhancement of Ca ions due to the destruction of dust grains by interstellar shocks.

4.5. Have we detected absorption components that can be associated with the expansion of the Cygnus Loop SNR?

From the discussion of the observations outlined in Sects. 4.1 to 4.4 we can summarize these results in five items: (i) the lines-of-sight towards stars with distances <300 pc produce single component absorption profiles with a velocity of $V_{\rm lsr} \sim 0$ km s^{-1} and a NaI/CaII density ratio ∼1–5, (ii) the sight-lines towards the six stars with distance estimates >500 pc (i.e. HD 197702, HD 198301, HD 198946, HD 199042, HD 199102 and HD 335212) produce absorption profiles that consist of two or three additional velocity components at $\sim V_{\rm lsr}$ = +9.0, +19.7 and +29.7 km s^{-1}, (iii) the physical size of the V_2 and V_3 gas (cloud) components is ∼20 pc, (iv) the NaI/CaII density ratio of these additional higher velocity components is typically <1.0, which is similar to values found for high-velocity gas components detected towards other SNRs, and (v) only red-shifted (positive velocity) absorption components have been detected.

From these results it would initially seem appropriate to associate these three additional, higher velocity components with an interaction between the expansion of the SNR and the surrounding ISM, since they have only been detected for distances estimated to be in excess of the 440 pc to the remnant. However, even allowing for sight-line projection effects, the velocities of these absorption components are very low in comparison with the shock velocities of ∼170 km s^{-1} derived from UV and visible emission line studies of the Cygnus Loop. However, the very high-velocity gas in Cygnus could be mostly in a state of high ionization and thus our present NaI and CaII observations (which sample gas <11.8 eV) would not be able to detect any expanding shells of hot, ionized gas. Although such a high ionization scenario is physically possible in SNRs, it would be highly unusual for the high-velocity expansion of the Cygnus SN not to have significantly affected the surrounding neutral interstellar medium (as is the case with the Monoceros Loop, Shajn 147 and Vela SNRs). We note however, that in a UV study of 45 stars in the vicinity of the Vela SNR only one-third of the targets revealed interstellar absorption components with velocities >60 km s^{-1} (Jenkins et al. 1984). Thus, in our present small sample of (6) stellar targets with distances >440 pc that have sight-lines that pass through the Cygnus Loop we may have been just unlucky not to find higher velocity absorption components.

In the diffuse ISM the majority of interstellar absorption components span a range in velocity of $\sim -20 < V < +20$ km s^{-1} for most of the sight-lines sampled within 300 pc of the Sun (Welsh et al. 1994). However, a few absorption components with velocities greater than ±30 km s^{-1} have also been detected towards these nearby stars (Welty et al. 1996; Welsh et al. 1994), and for sight-lines of even greater distance such high velocities become even more commonplace (Hobbs 1978). Thus, based solely on the observed magnitude of velocity of the NaI and CaII absorption components detected towards the Cygnus Loop we cannot confidently argue for their association with any global expansion of the SN shell and its interaction with surrounding interstellar gas. In fact, even for the Vela SNR in which far higher velocity absorption components were detected by Jenkins et al. (1984), these features were thought to be formed in individual shock-accelerated clouds rather than behind a SN shocked shell expanding into a uniform medium.

Furthermore, one may expect that a sight-line passing through the entire SNR would produce absorption components with *both* positive and negative velocities (i.e. components associated with the receeding and approaching shell

of the shock front). Thus, the fact that we have only detected red-shifted absorption components for sight-lines in excess of the 440 pc to the SNR would seem to argue against their association with a classically expanding remnant shell. However, we note that the Cygnus Loop SN is thought to have been formed in a pre-existing interstellar cavity, which could be the remains of a previous SNR (Braun & Strom 1986). The existence of pre-SNR shells is a common phenomenon and is thought to be the reason that most evolved SNRs are observable at all. In fact, it is the structure of this pre-cursor interstellar shell which is responsible for the morphological types found amongst evolved remnants. Since the NaI/CaII density ratios for the three higher velocity components are very low for typical diffuse interstellar gas and are more similar to those found in low-velocity shocked gas, a more likely explanation for the presently detected V_2, V_3 and V_4 absorption components is that they are associated with the original SN pre-cursor neutral shell material that may now have slowed down and formed interstellar sheets. We propose that high resolution UV observations of the sight-lines towards HD 198946, HD 198197 and HD 199042 would be particularly informative in determining: (a) if the elemental abundance and ionization state of the V_2, V_3 and V_4 components is consistent with that of an (old) pre-cursor SN neutral gas shell, and (b) if any high-velocity, high-ionization absorption components are present that could be associated with the high-velocity gas previously observed in emission towards the Cygnus Loop.

5. Conclusion

We have presented high resolution ($R \sim 5$ km s^{-1}) spectra of the NaI and CaII absorption lines observed towards 9 early-type stars of distances 250 to 2300 pc in the line-of-sight towards the Cygnus Loop SNR. All but one of these absorption profiles can be fit with a model consisting of a combination of one or more of three absorption components with average best-fit LSR velocities of $V_1 = +0.8$ km s^{-1}, $V_2 = +9.0$ km s^{-1} and $V_3 = 19.7$ km s^{-1}. An additional component at $V_4 = +29.7$ km s^{-1} is required to fit the NaI D1 and D2-line profiles recorded towards HD 198946.

We have found NaI/CaII density ratios of 1–5 for all the V_1 components, which are typical values found for diffuse neutral gas in the interstellar medium. For the higher velocity components a NaI/CaII ratio of <1.0 is generally found. Similarly low values have been derived by other authors for high-velocity gas components observed towards other evolved SNRs such as the Monoceros Loop, Shajn 147 and Vela SNR. These low ratios have been explained by an enhancement of CaII due to the removal of Ca ions from interstellar dust grains by interstellar shocks.

The higher velocity NaI and CaII absorption components have only been detected towards targets with distance estimates in excess of the 440 pc to the SNR. We find that the observed patterns of absorption are better explained if we assume distances of 600–800 pc for HD 198197, 500–600 pc for HD 199042 and ~550 pc for HD 335212.

We are unable to determine if the observed higher velocity components of V_2, V_3 and V_4 are associated with an interaction between the expansion of the Cygnus Loop SNR and the surrounding interstellar medium due to two main points: (i) the observed velocities of these components are very low in comparison with absorption features detected towards other evolved galactic SNRs, and (ii) only positive higher velocity components have been detected towards the Cygnus Loop whereas one may have expected additional higher velocity negative components associated with the approaching expanding shell of the SNR. Since the higher velocity components consist of cold and neutral gas with a NaI/CaII density ratio of generally <1.0, we suggest that they may be associated with a pre-existing neutral shell of shocked gas surrounding the interstellar cavity in which the Cygnus SN exploded some 20 000 years ago. We suggest that future high resolution UV absorption measurements of the lines-of-sight towards HD 198946, HD 198197 and HD 199042 would help clarify this issue.

Acknowledgements. This work was deemed unworthy of funding support by the NSF. We would like to thank Dr. John Vallerga and Dr. Bill Blair for important suggestions that have greatly improved this paper.

References

Balona, L., & Crampton, D. 1974, MNRAS, 166, 203
Blair, W., Raymond, J., Long, K., & Kriss, G. 1995, ApJ, 454, L35
Blair, W., Sankrit, R., Raymond, J., & Long, K. 1999, AJ, 118, 942
Braun, R., & Strom, R. 1986, A&A, 164, 208
Crawford, I. 1992, MNRAS, 259, 47
Danforth, C., Cornett, R., Levenson, N., Blair, W., & Stecher, T. 2000, AJ, 119, 2319
ESA, (1997), The Hipparcos and Tycho catalogues, ESA SP-1200, ESA Publications Division, Noordwijk
Gondhalekar, P., & Phillips, A. 1980, MNRAS, 191, 13
Graham, J., Levenson, N., Hester, J., Raymond, J., & Petre, R. 1995, ApJ, 444, 787
Hester, J., Raymond, J., & Blair, W. 1994, ApJ, 420, 721
Hobbs, L. 1978, ApJS, 38, 129
Humphreys, R., & McElroy, D. 1984, ApJ, 284, 565
Jenkins, E., Wallerstein, G., & Silk, J. 1984, ApJ, 278, 649
Klein, R., McKee, C., & Colella, P. 1994, ApJ, 420, 213
Ku, W., Kahn, S., Pisarki, R., & Long, K. 1984, ApJ, 278, 615
Levenson, N., Graham, J., Keller, L., & Richter, M. 1998, ApJS, 118, 541
Long, K., Blair, W. P., Vancura, O., et al. 1992, ApJ, 400, 214
McKee, C., & Ostriker, J. 1977, ApJ, 218, 148
Routly, P., & Spitzer, L. 1952, ApJ, 115, 227
Sankrit, R., Blair, W., Raymond, J., & Long, K. 2000, AJ, 120, 1925
Sfeir, D. M. 1999, Ph.D. Thesis, University of Paris 6
Silk, J., & Wallerstein, G. 1973, ApJ, 181, 799
Wallerstein, G., & Silk, J. 1971, ApJ, 170, 289
Welsh, B. Y., Craig, N., Vedder, P., & Vallerga, J. V. 1994, ApJ, 437, 638
Welsh, B. Y., Sfeir, D., Sallmen, S., & Lallement, R. 2001, A&A, 372, 516
Welty, D., Morton, D., & Hobbs, L. 1996, ApJS, 106, 533